

PAPER • OPEN ACCESS

## Benign termination of runaway electron beams on ASDEX Upgrade and TCV













To cite this article: U Sheikh *et al* 2024 *Plasma Phys. Control. Fusion* **66** 035003

View the [article online](#) for updates and enhancements.

You may also like

- [Scenario optimization for the tokamak ramp-down phase in RAPTOR: Part A. Analysis and model validation on ASDEX Upgrade](#)  
S Van Mulders, O Sauter, C Contré et al.
- [Energy gain of wetted-foam implosions with auxiliary heating for inertial fusion studies](#)  
R W Paddock, T S Li, E Kim et al.
- [Enhancement of fusion reactivity under non-Maxwellian distributions: effects of drift-ring-beam, slowing-down, and kappa super-thermal distributions](#)  
Haozhe Kong, Huasheng Xie, Bing Liu et al.

# Benign termination of runaway electron beams on ASDEX Upgrade and TCV

U Sheikh<sup>1,\*</sup> , J Decker<sup>1</sup>, M Hoppe<sup>2</sup> , M Pedrini<sup>1</sup>, B Sieglin<sup>3</sup> , L Simons<sup>1</sup>, J Cazabonne<sup>1</sup> , J Caloud<sup>4</sup>, J Cerovsky<sup>4</sup>, S Coda<sup>1</sup> , C Colandrea<sup>1</sup>, A Dal Molin<sup>5</sup> , B Duval<sup>1</sup>, O Ficker<sup>4</sup> , M Griener<sup>3</sup> , G Papp<sup>3</sup> , G Pautasso<sup>3</sup>, C Paz-Soldan<sup>6</sup> , C Reux<sup>7</sup> , E Tomesova<sup>4</sup>, T Wijkamp<sup>8</sup> , the ASDEX Upgrade Team<sup>9</sup>, the TCV Team<sup>10</sup> and the MST1 Team<sup>11</sup>

<sup>1</sup> Swiss Plasma Center (SPC), École Polytechnique Fédérale de Lausanne (EPFL), CH-1015 Lausanne, Switzerland

<sup>2</sup> Department of Electrical Engineering, KTH Royal Institute of Technology, Stockholm, Sweden

<sup>3</sup> Max Planck Institute for Plasma Physics, Boltzmannstr. 2, 85748 Garching, Germany

<sup>4</sup> Institute of Plasma Physics of the CAS, Za Slovankou 3, 182 00 Prague 8, Czech Republic

<sup>5</sup> Istituto per la Scienza e Tecnologia dei Plasmi, Consiglio Nazionale delle Ricerche, 20125 Milan, Italy

<sup>6</sup> Department of Applied Physics and Applied Mathematics, Columbia University, New York, NY 10027, United States of America

<sup>7</sup> CEA-IRFM, F-13108 Saint-Paul-les-Durance, France

<sup>8</sup> FOM Institute DIFFER 'Dutch Institute for Fundamental Energy Research', 5600 HH Eindhoven, Netherlands

E-mail: [umar.sheikh@epfl.ch](mailto:umar.sheikh@epfl.ch)

Received 20 September 2023, revised 20 November 2023

Accepted for publication 12 January 2024

Published 23 January 2024



CrossMark

## Abstract

This paper discusses the development of a benign termination scenario for runaway electron (RE) beams on ASDEX Upgrade and TCV. A systematic study revealed that a low electron density ( $n_e$ ) companion plasma was required to achieve a large MHD instability, which expelled the confined REs over a large wetted area and allowed for the conversion of magnetic energy to radiation. Control of the companion plasma  $n_e$  was achieved via neutral pressure regulation and was agnostic to material injection method. The neutral pressure required for recombination was found to be dependent on impurity species, quantity and RE current. On TCV,  $n_e$  increased at neutral pressures above 1 Pa, indicating that higher collisionality between the REs and neutrals may lead to an upper pressure limit. The conversion of magnetic energy to radiated energy was measured on both machines and a decrease in efficiency was observed at high neutral pressure on TCV. The benign termination technique was able to prevent any significant increase in maximum heat flux on AUG from 200 to 600 kA of RE current, highlighting the ability of this approach to handle fully formed RE beams.

<sup>9</sup> See author list of Stroth *et al* 2022 *Nucl. Fusion* **62** 042006.

<sup>10</sup> See author list of Reimerdes *et al* 2022 *Nucl. Fusion* **62** 042018.

<sup>11</sup> See author list of Labit *et al* 2019 *Nucl. Fusion* **59** 086020.

\* Author to whom any correspondence should be addressed.



Original Content from this work may be used under the terms of the [Creative Commons Attribution 4.0 licence](https://creativecommons.org/licenses/by/4.0/). Any further distribution of this work must maintain attribution to the author(s) and the title of the work, journal citation and DOI.

Keywords: runaways, disruptions, benign termination

## 1. Introduction

Disruption mitigation is the last line of defense against disruptions for a tokamak. Presently, it is achieved through massive material injection with the goal of radiating the stored thermal and magnetic energy over a large area. A bi-product of this process is an increase in plasma resistance and toroidal electric field, leading to an acceleration force on the electrons. This acceleration can overcome the collisional friction and result in the formation of relativistic electrons (RE). Current modeling predicts that an RE beam may be unavoidable during the nuclear phase of ITER [1–3].

If unmitigated, an RE beam has the potential to cause severe localized heating, which can lead to melting. This has already been observed on machines such as JET and at RE currents below 1 MA [4]. The conversion of magnetic energy to kinetic energy, and subsequently to heat flux at the RE impact location, is one of the key reasons for the destructive power of REs. Currently, there is no validated method for the safe termination of RE beams.

A potential solution for RE mitigation is ‘benign termination’ via low-Z injection and excitation of an MHD instability to expel the REs without regeneration [5]. The key to the success of this method is the conversion of magnetic energy to thermal energy and consequently radiated energy, thus spreading it over a large area. Prior to this work, this has only been explored on DIII-D, FTU and JET with promising initial results [6–8]. This paper outlines the application of this technique on ASDEX Upgrade (AUG) and TCV and a systematic study of its operational domain. Specifically, this paper will address the density regulation via neutral pressure as a function of impurity species, quantity and RE current, documentation of wetted area, and quantification of the conversion of magnetic to radiated energy. All with the final goal of creating a data set that can be used to develop models for the extrapolation of benign termination to ITER.

## 2. Benign termination scenario

The formation of a nominal RE beam on AUG and TCV is achieved via the injection of impurities into the plasma, as detailed in [9, 10]. Low density plasmas are used on both machines, with addition ECRH heating being applied on AUG to generate the seed population. A circular limited configuration was used on AUG, whilst an elongated and diverted plasma configuration was used on TCV. The injected impurities were Ar on AUG, and Ne, Ar and Kr on TCV for this study [11]. After the disruption and formation of the RE beam, a low temperature ‘companion’ plasma exists in parallel. The energy source for this companion

plasma is primarily collisions with the RE beam and energy is lost through radiation and conduction via neutrals. An overview of the benign termination process on AUG at varying RE currents is presented in figure 1, with the primary impurity injection indicated by the dashed cyan line. A non-benign termination example (red) is presented for comparison.

The first step in the benign termination sequence is the injection of low-Z material to increase the neutral pressure and recombine the companion plasma. This was achieved via D2 massive gas injection (MGI), indicated by the black dashed line in figure 1 at 1.02 s. At neutral pressures above this recombination threshold, the radiated power is reduced relative to the nominal RE beam scenario, indicating the companion plasma is predominantly cooled via conduction of energy to the walls via the neutrals [12]. If the D2 injection is insufficient, or the gas is pumped out, this will lead to a partially ionized companion plasma, as shown in the non-benign example (red) in figure 1.

An RE beam in the presence of a fully recombined companion plasma leads to a low RE loss rate, and subsequently system resistance, as evidenced by the low hard x-ray (HXR) signal (figure 1) and a reduction in loop voltage (not shown). The reduced loop voltage in turn leads to a reduction in the electric field and consequently the energy of the REs [13], as discussed in section 3.2.1. By applying the now available additional loop voltage, it is possible to increase the RE current until the desired value and allow for precise current scaling studies on AUG. This was not required on TCV due to full current conversion and a fixed current of 150 kA for this study. The current was not varied on TCV to allow gas species and quantity scans with minimal other variables.

The final stage in the benign termination process is the reduction of  $q_{\text{edge}}$  until an MHD instability grows, disrupting the plasma and expelling the confined REs. This is nominally achieved on AUG and TCV through compression of the plasma on the center column, as illustrated in figure 2. The fast expulsion of the REs leads to a spike on the HXR detector and current, indicating a re-connection event. The current is then carried by the cold Ohmic plasma, leading to high radiated power ( $P_{\text{Rad}}$ ) and a fast CQ. The radiated energy ( $W_{\text{Rad}}$ ) is indicative of the conversion of magnetic energy into radiation, preventing the conversion of magnetic energy into RE kinetic energy and subsequent heat-flux on plasma facing components [5].

The impact of the benign termination process on the disruption heat loads can be quantified via infrared (IR) thermography. The temperatures measured on the central column for both machines immediately following a benign and non-benign termination are shown in figure 3. The fields of view are approximately at the height of the magnetic axis on both machines with perpendicular (TCV) and tangential

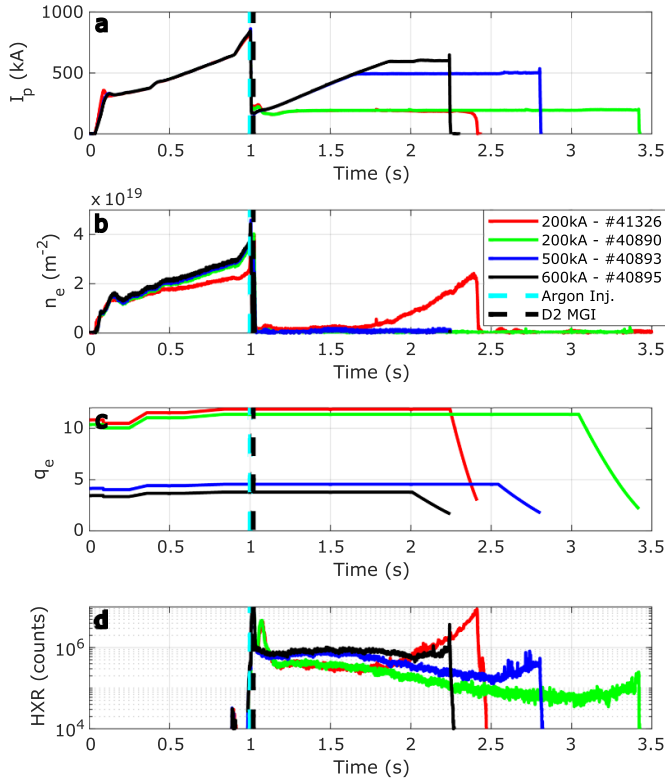


**Figure 1.** Overview of a non-benign (red) and benign termination pulses at 200, 500 and 600 kA on AUG.

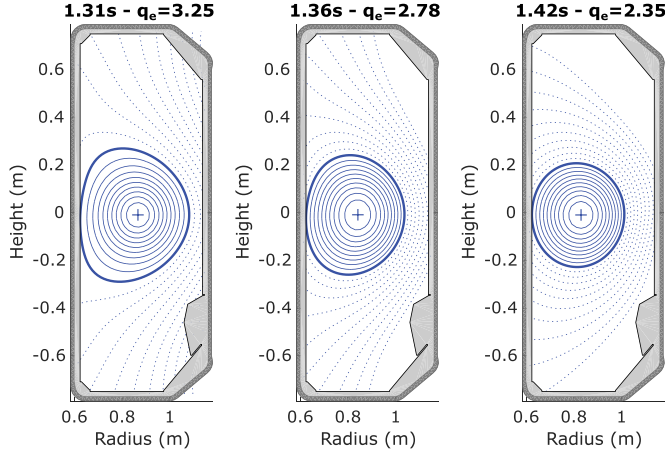


**Figure 2.** Compression of the plasma on the center column of TCV to approach low  $q_{\text{edge}}$  (#74638).

(AUG) views of the central column. The wider view on TCV demonstrates the large increase in wetted area and decrease in surface temperature achieved via the benign termination technique. The images from AUG, cropped to show the tile used for heat flux inferences in section 4, highlight the significant decrease in maximum surface temperature at the center of the beam impact. The full sequence of images showing increasing wetted area over the transition to benign termination are available in [12].

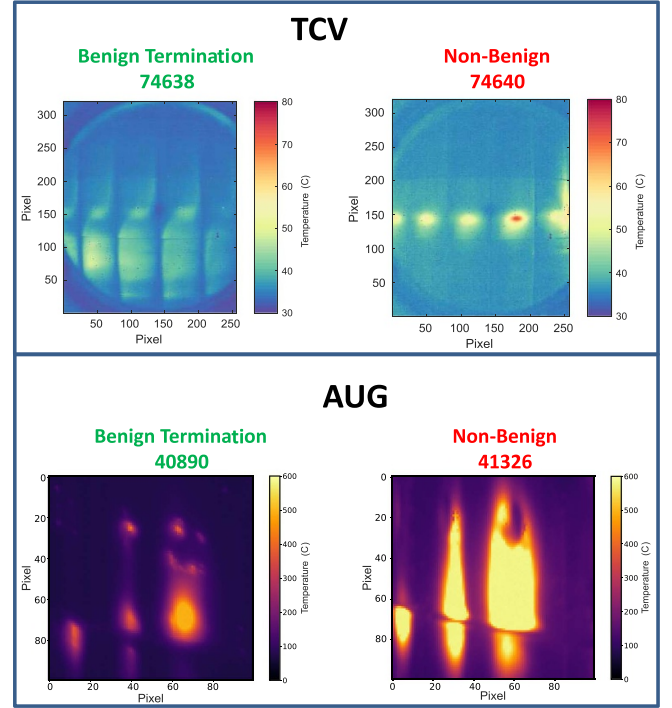


**Figure 3.** IR images of post-disruption center column tile temperatures on TCV (top) and AUG (bottom).

### 3. Operational domain

The operational domain of the benign termination scheme was explored through variations in the impurity gas species (Ne/Ar/Kr) and quantity injected to form the RE beam, low-Z gas species (H<sub>2</sub>/D<sub>2</sub>) and quantity, injection method, plasma current and the path to low  $q_{\text{edge}}$ . Fueling valves were used to maintain a desired neutral pressure when required, resulting in stabilization of the ionization rates and recombination rates for analysis.

The wetted area measured by the IR cameras was used as a proxy to gauge the effectiveness of the benign termination and spreading of the heat load. The wetted area was calculated by a count of the number of pixels above a threshold temperature, set by equation (1):

$$T_{\text{Threshold}} = T_{\text{Max.}} - 0.7(T_{\text{Max.}} - T_{\text{Avg.}}). \quad (1)$$

It was found that the wetted area increased with decreasing free electron density ( $n_e$ ), as shown in figure 4 top. This result suggests that recombination of the companion plasma is a prerequisite of benign termination. The neutral pressure was used to control  $n_e$  and was found to correlate directly with wetted area, figure 4 bottom. A rollover in wetted area was observed at neutral pressures above 0.5 Pa and this is addressed in section 3.2.

The nominal path to low  $q_{\text{edge}}$  in these experiments was compression of the plasma onto the center column. This will not be possible on ITER due to control system limitations

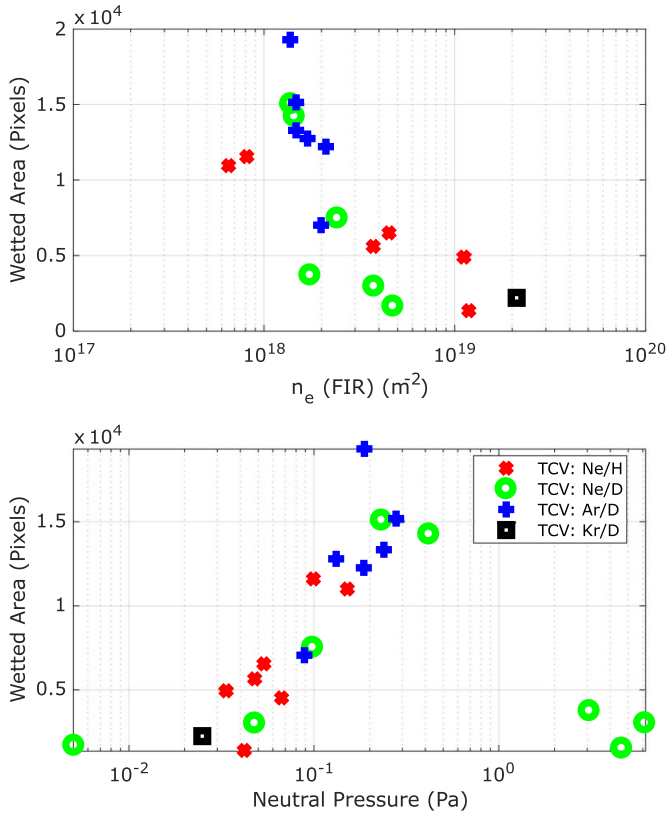


**Figure 4.** Post disruption wetted area inferences from an IR camera as a function of  $n_e$  (top) and neutral pressure (bottom).

[1]. Instead, a vertical displacement event (VDE) is expected to effectively compress the plasma until the MHD instability occurs. To explore the impact of variations in the path to low  $q_{\text{edge}}$ , compression rate scans were conducted on AUG and low  $q_{\text{edge}}$  was approached through  $I_p$  and  $B_T$  ramps on TCV. Compression rate scans doubling rate of compression and holding  $q_{\text{edge}}$  at integer values did not yield a clear result. All final collapses on AUG occurred at a  $q_{\text{edge}}$  of 2, with the exception of one disruption at  $q_{\text{edge}}$  of 3. Similarly, approaching  $q_{\text{edge}}$  via  $I_p$  and  $B_T$  ramps on TCV resulted in benign terminations occurring at a  $q_{\text{edge}}$  of 2 [12]. Attempts were made to vertically displace the beam on TCV, mimicking a VDE, and the current quench (CQ) rate and radiated power were characteristic of a benign termination. However, IR measurements to confirm this were not possible in this pulse due to the displacement of the beam. Partial collapses or re-avalanche of REs, as previously reported on JET [6], were not observed in these experiments.

### 3.1. Requirements for recombination

Having established that companion plasma recombination is required for benign termination, the minimum neutral pressures required to achieve this with different impurity species, quantity and plasma currents were explored. The gas species quantity scans were conducted on TCV and the plasma current scan on AUG. At plasma currents below 400 kA, sufficient

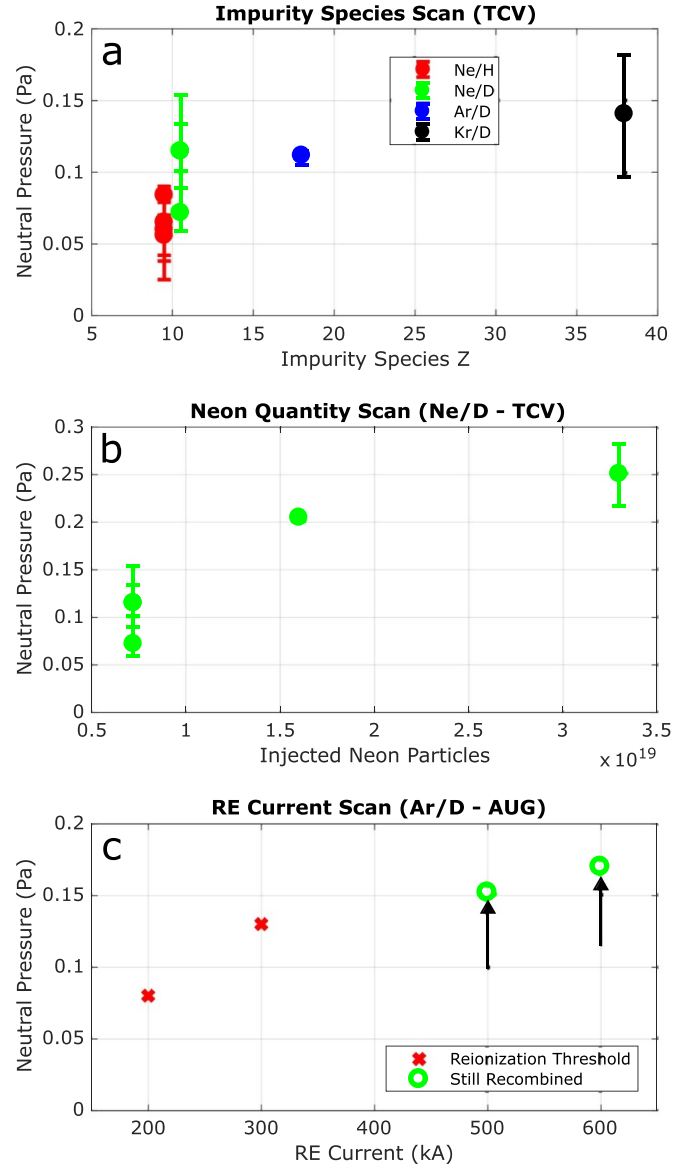


**Figure 5.** Neutral pressure requirements for recombination as a function of impurity species (a), neon quantity (b) and RE current (c).

H<sub>2</sub>/D<sub>2</sub> was injected to recombine the companion plasma and then pumped out until ionization was measured on the interferometer. The neutral pressure at which ionization occurred was identified as the minimum pressure required for recombination. At plasma currents above 400 kA, the neutral pressure was maintained slightly above the expected required neutral pressure, ensuring damage did not occur to the vessel via a non-benign termination of the beam.

Figure 5(a) presents the required neutral pressure for recombination of an RE beam created by an injection of  $7.2 \times 10^{18}$  impurity particles. The neutral pressure has been adjusted for delays in neutral conduction between the main chamber and the gauge, and the error bars indicate the neutral pressure 50 ms either side of the ionization time. It was found that a higher neutral pressure was required when higher-Z impurities

were used and the correlation is non-linear. Experiments substituting H2 for D2 showed a lower neutral pressure was required and this is attributed to H2's relatively higher energy conduction.

Increasing the quantity of neon injected, figure 5(b), or the RE current, figure 5(c), also led to an increase in the neutral pressure required for recombination. This is attributed to higher collisionality between the REs and impurities, leading to higher energy transfer from the REs to the companion plasma. The quantity scaling was found to be non-linear and the current threshold did not scale as a quadratic, as expected by Ohmic power. A power balance model is being developed to interpret these results and extrapolate to larger machines.

### 3.2. Neutral pressure upper limit

Inability to achieve benign termination at high neutral pressure has been previously observed on DIII-D [14] and was also observed on TCV during these experiments. No upper limit was found on AUG up to a maximum neutral pressure of 0.75 Pa at 200 kA. Dedicated discharges on TCV with stable post-secondary injection conditions for 200 ms were conducted to explore this phenomena. Plasma parameters were averaged across this time window to identify any potential small changes in  $n_e$  measured by an interferometer (FIR) and a low temperature Thomson Scattering chord at 9.7 cm above the magnetic axis.

The results of this study, figure 6, clearly indicate that an increase in companion plasma  $n_e$  is observed at high neutral pressures, whilst  $T_e$  continues to decrease. This is attributed to an increase in the ionization rate through collisions between REs and neutrals. The lower  $T_e$  indicates that conduction of energy through neutrals to the walls continues to increase. Measurements above 3 Pa were not possible due to the lower limit of the Thomson Scattering system. This hypothesis is explored in the following section through spectroscopic inferences.

**3.2.1. Spectroscopic inferences.** Broadband spectral measurements obtained for high neutral pressure discharges during the post D2 injection stable time intervals described in the previous section are presented in figure 7. These measurements were made with a vertical view line at the center of the vessel. A low neutral pressure benign termination case is overlaid in red for comparison. An increase in continuum spectra at wavelengths below 656 nm and above 860 nm was measured at high neutral pressure. Electron-ion recombination is expected to become important for radiation emission at  $T_e$  below approximately 1 eV, which occurs at neutral pressures above 1 Pa. Thus, it is hypothesized that the ionization rate has increase due to the number of collisions between the REs and the increased density of neutral targets. Coupled with the sub 1 eV  $T_e$ , the number of electron-ion recombination reactions has also increased. This in turn leads to the observed increase in continuum emission below 656 nm and the immediate cutoff at higher wavelengths or lower energies.

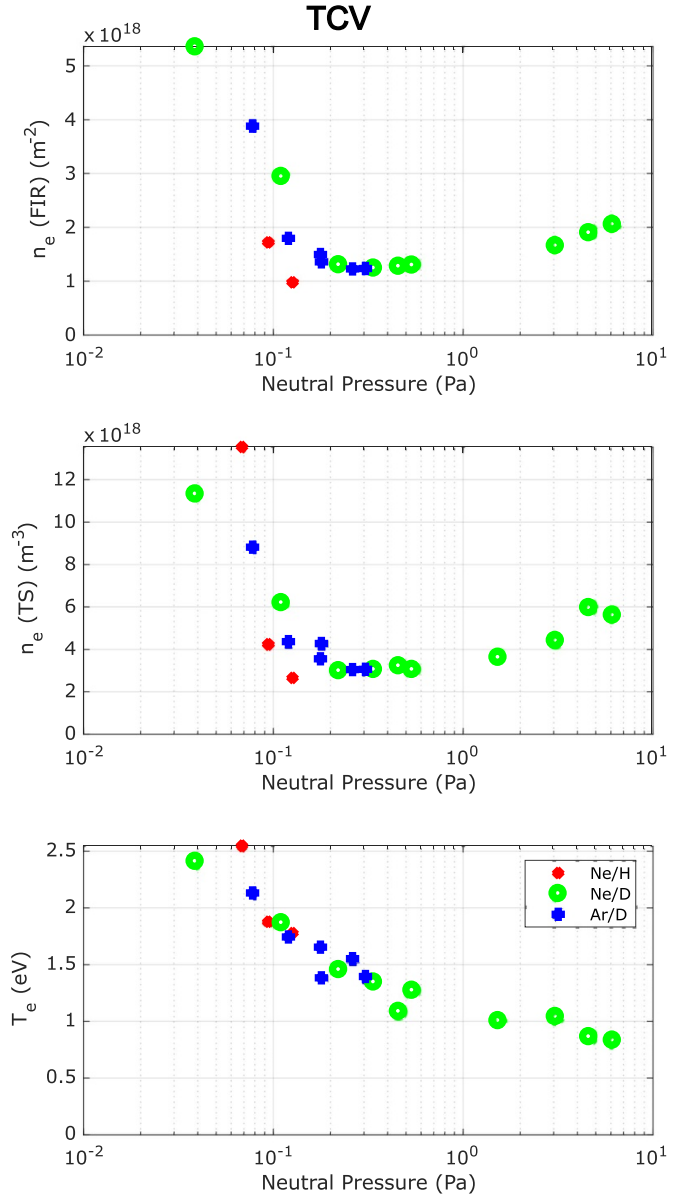


**Figure 6.** Companion plasma  $n_e$  and  $T_e$  as a function of neutral pressure on TCV.

Further evidence of increased energy transfer from the RE beam to neutrals at high neutral pressure was the rise in loop voltage. The increased loop voltage results in a higher electric field, which in turn increases the energy of the REs. Measurements of HXR photons at detectors positioned outside the torus hall, shown in figure 8, provide qualitative evidence of an increase in RE energy when the companion plasma is not recombined or if there is a high neutral pressure [15, 16]. A decrease in HXR photon energies and counts is observed at neutral pressures sufficient for recombination but still below 1 Pa on both AUG and TCV. An increase in RE energy is not expected to be a limiting factor in the benign termination process as the plasma current ramp up, which required a higher loop voltage, was still successful.

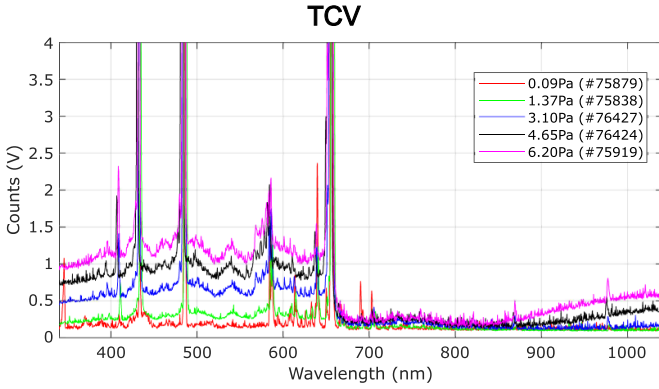


**Figure 7.** Spectra from high neutral pressure discharges and a low neutral pressure benign termination case on TCV (red).

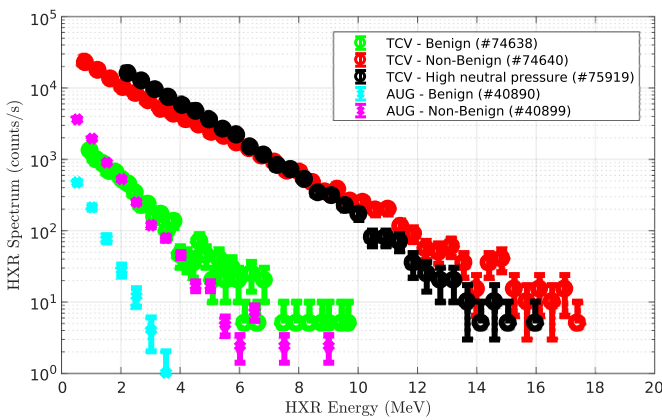


**Figure 8.** HXR photon spectra measured ex-vessel on AUG and TCV.

#### 4. Final collapse

A large mode growth rate is expected at the onset of the final MHD instability used to expel the REs, resulting in a highly radiating plasma which converts magnetic energy to radiated energy. The large growth rate is ascribed to the high Alfvénic velocity achievable in a low  $n_e$  plasma, which in turn sets the requirement for a low  $n_e$  companion plasma to achieve benign termination. The mode growth rate was inferred from magnetic probe measurements on both machines. In-vessel probes on the central column that were vertically closest to the magnetic axis without saturating were used for this analysis. Figure 9 top indicates the mode growth rate follows a similar trend to the wetted area on TCV: increasing until a maximum at approximately 0.5 Pa before decreasing at higher neutral pressures. The measurements on AUG also show an increase in mode growth rate with increasing neutral pressure. There is however large scatter at 0.1 Pa and this is attributed to limited measurement capabilities due to strong saturation of magnetic probes close to the collapse.

Expulsion of the REs and transfer of the current to the cold companion plasma results in fast CQ rates, as shown in figure 9 bottom. Measurements with the HXR spectroscopy system

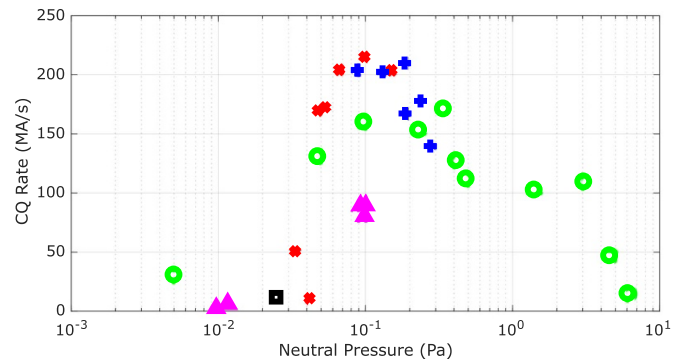
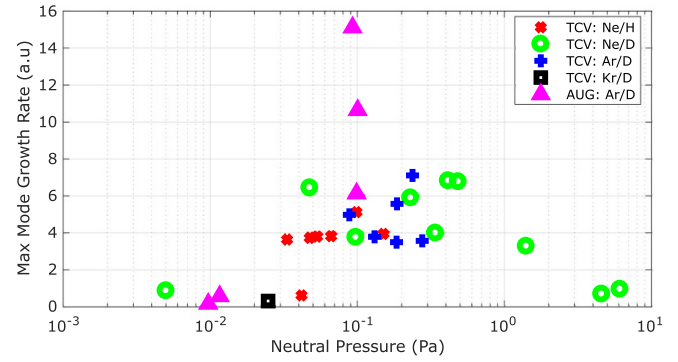


**Figure 9.** Maximum mode growth rate (top) and CQ rate (bottom) as a function of neutral pressure.

indicate the last HXR photon measured occurred at over 98% of the nominal RE current prior to mode peak amplitude on TCV for all CQ rates above  $100 \text{ MA s}^{-1}$ . The peak CQ rate, however, was achieved at neutral pressures below the peak mode growth rates, indicating sub-optimal growth rates may be sufficient to expel the entire RE population. The reduction in CQ rate at higher neutral pressures is not yet understood.

The conversion of magnetic energy to radiated energy was inferred through bolometric measurements and is presented in figure 10. In standard disruption sequences, bolometer measurements are too slow to distinguish between emission during the thermal quench and CQ. However, since there is effectively no kinetic energy in these plasmas, all emission from the start of the CQ can be deemed to be magnetic energy and thus the inference is simplified. Increasing radiated energy during the CQ was observed with increasing CQ rate and neutral pressure, until a rollover at high neutral pressure. This result clearly demonstrates the conversion of stored magnetic energy to radiated energy via the benign termination technique on both machines.

The total stored magnetic energy increases quadratically with increasing plasma current and its influence on radiated energy during the CQ on AUG is presented in figure 11 top. Almost an order of magnitude more energy is radiated at 200 kA when the neutral pressure is increased and benign termination is achieved (red). This in turn leads to a 3x decrease in maximum heat flux inferred from the IR cameras (figure 11 bottom) [12]. As the plasma current is increased to

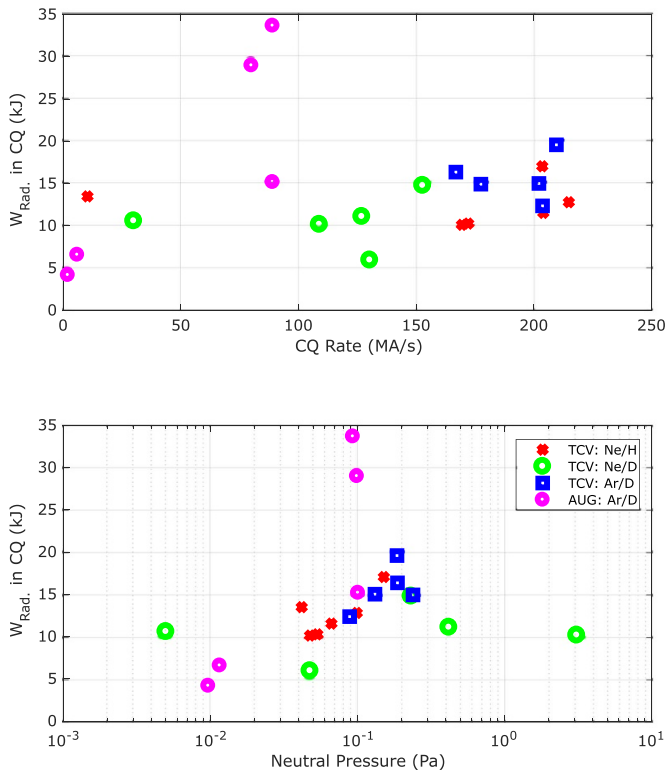


**Figure 10.** Radiated energy during the CQ as a function of CQ rate (top) and neutral pressure (bottom). AUG data only at 200 kA shown.

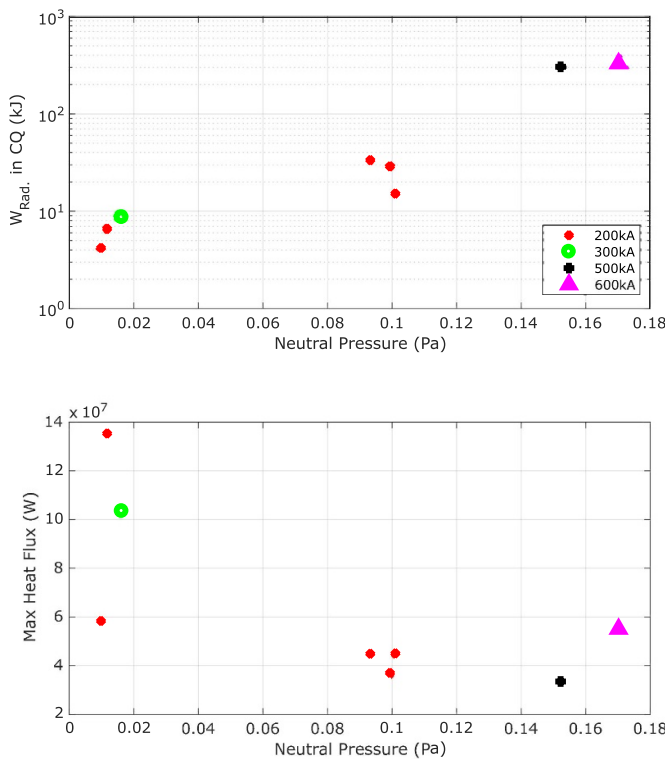


**Figure 11.** Radiated energy (top) and maximum heat flux (bottom) as a function of neutral pressure and plasma current (colors and symbols) on AUG.

500 and 600 kA, an increase in radiated energy of approximately another order of magnitude is measured. Conversely, the maximum heat flux does not increase significantly, highlighting the success of the benign termination technique at high currents.

### 5. Conclusions

This study has developed the benign termination technique for REs on AUG and TCV, and explored its operational space in a systematic manner. It was found that benign termination requires a low  $n_e$  companion plasma, which is achieved through cooling via neutral conduction. The minimum neutral pressure for recombination was found to be a non-linear function of injected impurity species, quantity and plasma current. An upper limit in neutral pressure was observed and attributed to increasing collisions between the REs and neutrals, leading to a rise in  $n_e$ . Benign termination was agnostic to the low-Z material injection method and path to low  $q_{\text{edge}}$ . Complete expulsion of REs and conversion of the stored magnetic energy to radiated energy was observed at the final collapse. The efficacy of this conversion was linked to mode growth rate and neutral pressure at the time of collapse. Sub-optimal mode growth rates were still able to produce benign termination and a reduction in CQ rate was observed at neutral pressures above 0.3 Pa on TCV. This technique was successfully used at RE currents of up to 600 kA on AUG with maximum heat fluxes below a non-benign termination at 200 kA.

### Data availability statement

The data cannot be made publicly available upon publication because no suitable repository exists for hosting data in this field of study. The data that support the findings of this study are available upon reasonable request from the authors.











### Acknowledgments

This work has been carried out within the framework of the EUROfusion Consortium, partially funded by the European Union via the Euratom Research and Training Programme (Grant Agreement No. 101052200—EUROfusion). The Swiss contribution to this work has been funded by the Swiss State Secretariat for Education, Research and Innovation (SERI). Views and opinions expressed are however those of the author(s) only and do not necessarily reflect those of the European Union, the European Commission or SERI. Neither the European Union nor the European Commission nor SERI can be held responsible for them. C Paz-Soldan acknowledges support from US DOE under DE-SC0022270.

### ORCID iDs

U Sheikh <https://orcid.org/0000-0001-6207-2489>  
 M Hoppe <https://orcid.org/0000-0003-3994-8977>



B Sieglin  <https://orcid.org/0000-0002-9480-4434>  
 J Cazabonne  <https://orcid.org/0000-0001-7629-1375>  
 S Coda  <https://orcid.org/0000-0002-8010-4971>  
 A Dal Molin  <https://orcid.org/0000-0003-0471-1718>  
 O Ficker  <https://orcid.org/0000-0001-6418-9517>  
 M Griener  <https://orcid.org/0000-0003-2953-536X>  
 G Papp  <https://orcid.org/0000-0003-0694-5446>  
 C Paz-Soldan  <https://orcid.org/0000-0001-5069-4934>  
 C Reux  <https://orcid.org/0000-0002-5327-4326>  
 T Wijkamp  <https://orcid.org/0000-0003-3110-8682>

## References

- [1] ITER Physics Expert Group on Disruptions, Plasma Control and MHD and ITER Physics Basis Editors 1999 Chapter 3: MHD stability, operational limits and disruptions *Nucl. Fusion* **39** 2251
- [2] Lehnen M *et al* 2015 Disruptions in ITER and strategies for their control and mitigation *J. Nucl. Mater.* **463** 39–48
- [3] Vallhagen O, Pusztai I, Hoppe M, Newton S L and Fülöp T 2022 Effect of two-stage shattered pellet injection on tokamak disruptions *Nucl. Fusion* **62** 112004
- [4] Matthews G F *et al* 2016 Melt damage to the JET ITER-like Wall and divertor *Phys. Scr.* **2016** 014070
- [5] Paz-Soldan C, Eidietis N W, Liu Y Q, Shiraki D, Boozer A H, Hollmann E M, Kim C C and Lvovskiy A 2019 Kink instabilities of the post-disruption runaway electron beam at low safety factor *Plasma Phys. Control. Fusion* **61** 054001
- [6] Paz-Soldan C *et al* 2021 A novel path to runaway electron mitigation via deuterium injection and current-driven MHD instability *Nucl. Fusion* **61** 116058
- [7] Carnevale D *et al* 2021 Results on quiescent and post-disruption runaway electrons studies at Frascati Tokamak Upgrade: RE mitigation via solid deuterium pellets and anomalous Doppler instability *Nucl. Fusion* **61** 116050
- [8] Reux C *et al* 2021 Demonstration of safe termination of megaampere relativistic electron beams in tokamaks *Phys. Rev. Lett.* **126** 175001
- [9] Decker J *et al* 2022 Full conversion from ohmic to runaway electron driven current via massive gas injection in the TCV tokamak *Nucl. Fusion* **62** 076038
- [10] Pautasso G *et al* 2016 Disruption mitigation by injection of small quantities of noble gas in ASDEX Upgrade *Plasma Phys. Control. Fusion* **59** 014046
- [11] Sheikh U A *et al* 2020 Runaway electron studies and plasma restart from a RE beam on TCV *IAEA Technical Meeting on Plasma Disruptions and Their Mitigation (Virtual Meeting)*
- [12] Sheikh U A *et al* 2023 Benign termination of runaway electron beams in the Eurofusion tokamak exploitation workprogram *Proc. of the IAEA FEC (London, 16–21 October 2023)*
- [13] Pavel A and Breizman B N 2015 Theory of two threshold fields for relativistic runaway electrons *Phys. Rev. Lett.* **114** 155001
- [14] Hollmann E M *et al* 2020 Study of argon expulsion from the post-disruption runaway electron plateau following low-Z massive gas injection in DIII-D *Phys. Plasmas* **27** 042515
- [15] Simons L *et al* 2023 Design of a Lanthanum Bromide detector for Runaway Electrons on TCV *Rev. Sci. Instrum.* submitted
- [16] Dal Molin A *et al* 2023 A new hard x-ray spectrometer for runaway electron measurements in tokamaks *Meas. Sci. Technol.* **34** 085501